NOVATEUR PUBLICATIONS
INTERNATIONAL JOURNAL OF RESEARCH PUBLICATIONS IN ENGINEERING AND TECHNOLOGY [IJRPET]
NATIONAL CONFERENCE ON INNOVATIVE TRENDS IN ENGINEERING & TECHNOLOGY-2017
15TH & 16TH MARCH 2017
CONFERENCE PROCEEDINGS ISSN NO - 2454-7875

Paper ID: NITET04

SYNTHESIS, CHARACTERIZATIONS AND TRIBOLOGICAL EVALUATION OF NANOCRYSTALLINE HYDROXYAPATITE AND NOVEL WILLEMITE.

NARESH P. PATIL
Department of Mechanical Engineering, A. G. Patil Polytechnic Institute, Solapur.

SHRIKANT R. DAWANKAR
Department of Mechanical Engineering, A. G. Patil Polytechnic Institute, Solapur.

VILAS G. AMBIGAR
Department of Mechanical Engineering, A. G. Patil Polytechnic Institute, Solapur.

ABSTRACT

Bioceramics are potentially attractive for a wide range of medical and mechanical applications. In the present investigation Hydroxyapatite (HA) and Willemite (WM)were successfully prepared by sol-gel auto combustion and sol-gel methods respectively. The prepared materials were characterized by X-ray Diffraction (XRD), Scanning Electron Microscopy (SEM), Energy Dispersive Spectroscopy (EDS) and Transmission Electron Microscopy (TEM). Friction and wear characteristics of HA and WM were determined using a pin-on-disc tribometer at applied loads in the range of 50N -110N. Results reveal that the wear performance of HA was superior to WM also possess lower friction coefficients than WM. To calculate the wear depth by Archard wear model FEA is done. It was observed that no significant difference between experimental and numerical wear depth.

INDEX TERMS: Biomedical applications, FEA, Hydroxyapatite, Pin-on-disc, Solution Combustion, Sol-gel, Tribology, Willemite.

INTRODUCTION

Bio-ceramic is an important subset of biomaterial which is used for replacing and damaged part of the musculoskeletal system. The importance of Bio-ceramics in biomedical applications has been universally accepted as they show an excellent biological, mechanical and biochemical properties [1]. Bio-ceramics can be divided into two large groups: Bio-inert ceramics and bioactive ceramics [2]. Bio-inert ceramics show no influence on the surrounding living tissues whereas bioactive ceramics are able to bond with living tissues. Hydroxyapatite (HA) and Willemite (WM) are two bioactive ceramics.

Hydroxyapatite $Ca_{10}(PO_4)_6(OH)_2$ has excellent biocompatibility and surface active properties with living tissues, it has become one of the most important bio-ceramic materials for artificial bone [3]. The chemical composition of bone is similar to HA [4]. HA is a one of the main constituents of bone cement, but due to its brittleness and poor strength, HA restrict its bio-medical applications under load and friction conditions [5]. Joints grafting such as knee, hip is an effective surgical treatment to relieve pain and to restore the locomotion function for patients with unused joints. An ideal bone implant should be osteoinductive, resorbable, easy to shape and possessing adequate mechanical properties [6]. Artificial HA is widely used in bone tissue engineering [7, 8]. HA is also used as ion-exchanger, catalyst and adsorbent [9-11]. In addition to these recent studies proved that HA particles were used for anti-cancer treatment [12]. Willemite (WM), Zn_2SiO_4, also known as zinc orthosilicate, is the main constituent of crystalline glazes seen in modern day pottery [13]. WM is also known as Glass ceramics. Glass ceramics such as WM having good mechanical strength, high colour purity, high luminescence efficiency strong chemical durability, and highly thermal stabilities and these properties are suitable for different applications [14-15]. WM exists in three different phases which are □□□□ and □-Zn_2SiO_4 and shows three different colours of emission:□□-Zn_2SiO_4 (green Emission), yellow emission (□-Zn_2SiO_4), and red colour (□ -Zn_2SiO_4). In the earth's crust Silicate minerals are found abundantly. Research on WM ceramics have been considered to be technologically and biologically important; because of the extraordinary properties of materials possess electrical conductivity, good mechanical strength, thermal conductivity, dielectric properties and a low coefficient of thermal expansion [16]. They are ionic crystals; possess tetrahedral SiO_4 or complex molecules formed by the coupling of SiO_4 tetrahedral. From one to five valence cations can be bonded to produce a very large variety of silicate crystals [17]. Pure WM is a silicate of individual unlinked silicon tetrahedral. Each zinc atom is also at the centre of the oxygen tetrahedral of almost the same size as that of silicon tetrahedron. Every oxygen atom has one silicon and two zinc atoms at the corners of a triangle. Potential fields of application for WM are pharmaceutics or biological, optoelectronics, optics and medical diagnostics [18-20].

Tribology is a branch of science and technology of interacting surfaces in relative motion. There are three parameters of tribology friction, wear and lubrication [21]. The tribological behaviour of HA investigates by many works. Qian Zhao et al [22] studied the effect of CNT addition on coefficient of friction of HA composites against a stainless-steel ball. Zhi Lu et al [23] analyzed micro-

tribological properties of HA-based composites in ball-on-block tribometer and describe the relationship between the load and the wear resistant. J. Zheng et al [24] micro-tribological properties of artificial HA and human tooth enamel and found an enamel having significant plastic deformation than HA at low load

HA has been synthesized by many routes, including co-precipitation [25], sol–gel synthesis [26], emulsion methods [27], microwave precipitation [28] and mechanochemical methods [29]. A large number of research efforts have been focused toward the preparation of important materials, mostly oxides with improved properties by using the solution combustion method [30]. In solution combustion synthesis, aqueous reactive solutions are used, where the precursors are mixed on the molecular level. The advantage of this process has been demonstrated by the use of different fuels and oxidizers, varying the oxidizer/fuel ratio and ignition sources, as well as a combination of various synthesis approaches [31]. Willemite has been synthesized by many routes, such as hydrothermal method [32], ball mill [33], solid-state reaction method [34] and sol–gel synthesis [35]. Sol-gel synthesis method has lowest processing temperature method and performed with solvents such as alcohol, ionic liquid and water. The significance of sol-gel methods are it is performed in a solvent at ambient pressure, while in solvothermal and hydrothermal methods tend to use high pressures and high temperatures. Sol-gel literature shows that crystallization of Zn_2SiO_4 requires at least temperatures of around 100^0C. Sol-gel methods have the advantage of providing characteristic particles such as spherical particles, uniform shapes, or Nano-sized particles by varying the some experimental conditions; they may be combined with the other synthesis routes in the future [36].

In the present study, HA and WM were prepared by sol-gel auto combustion and a sol-gel method respectively. This works aims to study the tribological parameter of HA and WM under different loading condition on pin-on-disc tribometer. To prepare a pin of HA and WM acrylic material used .The (90:10) composition were used to prepare a pin. To find pressure distribution on pin FEA is done. Archard wear model is used to find the wear depth numerically.

EXPERIMENTAL

A. CHEMICALS USED

For synthesis of Willemite Tetraethylorthosilicate (Si $(OC_2H_5)_4$; TEOS, Sigma-Aldrich and purity ≥99%), Zinc chloride ($ZnCl_2$, Thomas baker AR grade), HCL and distilled water used and Calcium nitrate tetra hydrate (Ca $(NO_3)_2.4H_2O$, Thomas baker AR grade), di-Ammonium hydrogen orthophosphate ($(NH_4)_2HPO_4$, Thomas baker AR grade) and polyvinyl alcohol (PVA, Thomas baker AR grade) used for Hydroxyapatite. All chemicals used here were of analytical grade and used without further purification.

B. SYNTHESIS OF HYDROXYAPATITE

Hydroxyapatite (HA) was prepared by modifying solution combustion method. For this, polyvinyl alcohol (PVA) was used as a fuel. In brief, the stoichiometric amounts of the nitrate precursors Ca $(NO_3)_2.4H_2O$, and phosphate precursor $(NH_4)_2HPO_4$ were dissolved in double distilled water to form the solution of 0.1 M. The equimolar solution of PVA was prepared in double distilled water. The mixture of oxidants and fuel was placed onto a magnetic stirrer for 30 min to get uniform mixing. Evaporation of water to form a gel of precursors was carried out at 100 °C and then the gel was heated at 300°C to obtain a powder. The obtained powder of HA was then annealed at 950 °C for 6 h to remove carbon residues and then used for further analysis. The dried mixture possesses the characteristics of combustion and can be ignited to start the combustion reaction using muffle furnace. This method is reported previously by researcher [37].

C. SYNTHESIS OF WILLEMITE

Willemite (WM) was synthesized by sol-gel method. Tetraethylorthosilicate ($Si(OC_2H_5)_4$) was first partially hydrolysed at a molar ratio of TEOS: water:=2.40:0.25 and HCL was used as a binder in the solution. 2 mol zinc chloride was dissolved in pre-hydrolyzed solution. This solution was stirred by a magnetic stirrer to form a homogeneous solution. After completion of stirring the solution was refluxed around 35^o C until the gel formation. Gel was dried in the oven at 300^o C. The resulting powder was then annealed in the temperature range of 500°–1200^o C for 2h with a heating rate of 5°C min. This method was reported previously by researcher [38]

D. CHARACTERIZATIONS

The structural and morphological studies of the samples were studied using X-ray Diffractometer (XRD), Transmission Electron Microscopy (TEM) and Scanning Electron Microscopy (SEM).Phase identification and structure analysis of Hydroxyapatite and Willemite were studied using X-ray diffraction (Philip-3710) with Cu-Kα radiation in the2θ range from 10^0 to 60^0. The pattern was analysed by X-pert High score plus software and compared with the Joint Committee on Powder Diffraction Standards (JCPDS) (JCDPS card no.01-074-0565 and 01-075-0278). The surface morphology and particle sizes of the Hydroxyapatite and Willemite were determined by using transmission electron microscope (Philips CM 200 model) with an operating voltage of 20–200 kV and a resolution of 2.4Å.The compositional analysis was done by energy dispersive spectroscopy (EDS, JEOLJSM 6360).

E. WEAR TEST

Tribological parameters were carried out using a pin-on-disc Tribometer [39]. The image of tribometer used was shown in Fig. 1. HA and WM were used as the friction material as well as gray cast iron material was used for the disc. The size of the disc was 165 mm in diameter, 8 mm in

thickness and the hardness of 62 HB. The normal load was applied to pin through loading lever which was a single bar with specimen holder fixed at one end and at another end it has a wire rope for suspending dead weight to apply normal load. Rotational speed and time of revolution were applied through controller, which was connected to a machine. The disc was connected to motor through a variable speed clutch capable of imparting speed up to 2000 rpm to the disc. The LVDT (Linear Variable Differential Transducer) and load cell measure wear and frictional force which was displayed on the controller. Graphical representation of wear and frictional coefficient were visible on a PC. The frictional surface of the disc was abraded with a 320 grade abrasive paper and was cleaned by a dry cloth before each test in order to start with same surface roughness.

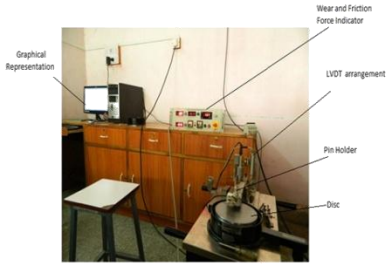

Fig. 1.Pin on disc tribometer.

F. PIN PREPARATION

The nanoparticles of HA and WM were used for pin preparation. Here powder of ceramic material and acrylic repair material (90:10) were used for pin preparation, when they were mixed together formed a semisolid mass. This semisolid mass was pressed in a die by UTM at 0.3 ton load. Formed pins have 10 mm diameter and 20 cm in length.

RESULTS AND DISCUSSION

A. XRD ANALYSIS

The X-ray diffraction (XRD) pattern of the pure HA was given in Fig. 2 (a). XRD spectra were recorded in the 2 theta range 10-60o and step size of 0.02. The main phase, in the samples was identified as Hydroxyapatite (JCDPS No.01-074-0565). The crystallite size of HA was calculated from full width half maximum of the strongest diffraction peak using Debye-Scherer formula [40]. The crystallite size of HA is 34.50 nm. For pure HA similar results and phase purity were observed in reported work [41-42]

The XRD pattern of the pure WM samples was shown in Fig. 2 (b).The main phase, in the sample was identified as Willemite (JCDPS no. 00-037-1485). There were no secondary phases observed in the sample. Willemite showed a rhombohedral structure with space group R-3.It can be seen that, the lattice parameters of the prepared sample were in excellent agreement with standard data a=13.93 Å, c=9.3100 Å. The crystallite size of Willemite was calculated from full width half maximum (FWHM) of the strongest diffraction peak using Debye-Scherer formula [40]. The crystallite size of Willemite was 38.42nm. About Willemite similar results were observed in reported work [43].

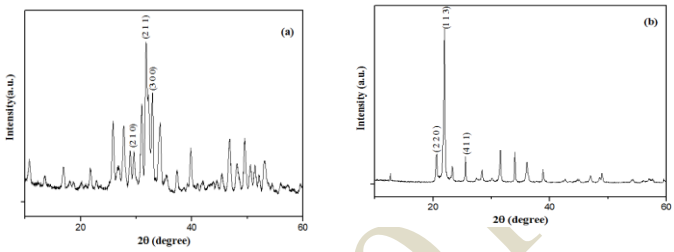

Fig. 2.XRD patterns of (a) HA and (b) WM

B. SEM ANALYSIS

The Scanning electron Microscopy (SEM) technique was used to observe and analyse the microstructure, agglomeration and particle size of HA and WM. In Fig. 3 (a) and (b) SEM micrographs of hydroxyapatite samples were shown similar agglomerates that were consisting of fine crystallites. SEM micrographs of WM show Rod like crystalline structure with an average length of less than 50µm.

Composition analysis of pure HA and WM was carried out by EDS technique. The EDS pattern for pure HA and WM was shown in Fig. 4 (a) and (b) and the detail composition was given in Table. 1. From the data it was confirmed that HA was composed of Ca, P, O &WM was composed of Zn, Si and O. The Ca/P atomic ratios in HA was 1.69 which was near about the standard 1.67[1].

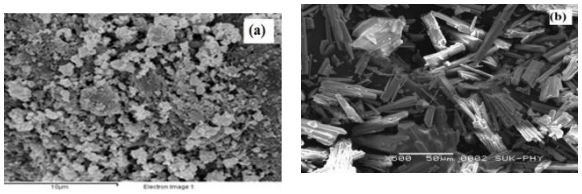

Fig. 3. Scanning electron microscopy (SEM) images of a) HA and b) WM

Table. 1 Atomic percentage composition

Name	Ca	P	O
Hydroxyapatite	38.68	22.89	38.43
Name	Zn	Si	O
Willemite	14.23	20.58	58.15

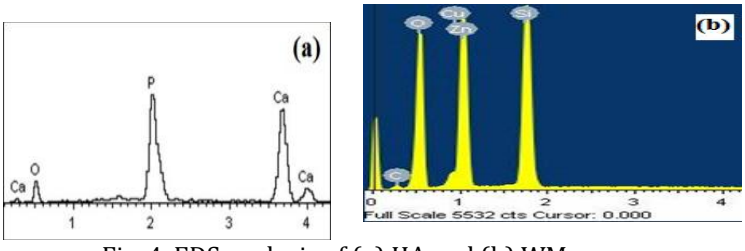

Fig. 4. EDS analysis of (a) HA and (b) WM

C. TEM STUDIES

The particle size of HA and WM were estimated from TEM analysis. Fig. 5 (a) and (b) show TEM micrographs of HA and WM. The HA and WM nanoparticles were possessing a cylindrical rod-like shape with homogeneous microstructure. HA particles have size less than 100 nm in diameter. However, the WM particles have size around 200 nm in diameter. The diameters of the particles were slightly larger than the observed crystal sizes obtained from XRD, due to the high-temperature calcination which causes the grain growth. The corresponding SAED pattern (inset of Fig. 5 (a) and (b)) show bright ring patterns indicating the polycrystalline nature of nanoparticles, which were in good agreement with XRD results.

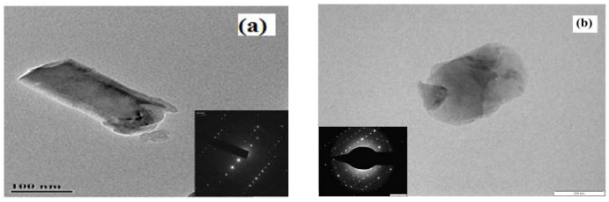

Fig. 5 TEM images of (a) HA and (b) WM (Inset: corresponding SAED pattern.).

TRIBOLOGY TEST

The variation of friction coefficients of HA and WM with sliding distance under different loads was shown in Fig. 6 (a) and (b), respectively. It can be seen that HA showed lower coefficients at the low load and it increases with the increasing load. It was seen that there was gradual increase in the friction coefficient of HA with increased sliding distance. On the other hand, WM exhibits different behaviour with its friction coefficient increasing gradually first and then decreasing over the sliding distance. The friction coefficients for WM were constant for 70 and 110 N at 100 and 250 m and at 366 m constant for 70 and 90 N. Friction coefficients of WM at 50 and 110 N have less fluctuation. From both the graphs, it is clear that the friction coefficient of both material increase as load increase over a sliding distance.

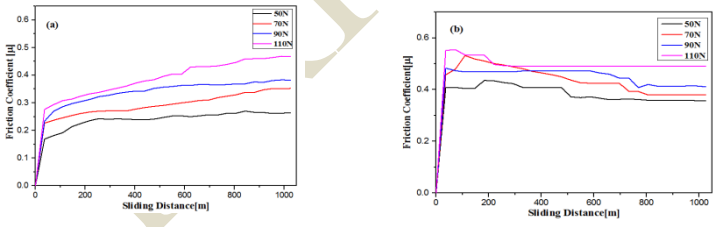

Fig. 6 Friction coefficients of (a) HA and (b) WM

Table 2. present a summary of the average values of friction coefficients and Wear rate. Wear rates for HA and WM were shown in Fig. 7. It was clear that wear rate of WM was higher than HA, which was in agreement with their high friction coefficient of friction values. The wear rates of both the material were increased with increase in applied load.

Table.2. Comparison of Friction Coefficient and Wear rate of HA and WM

Load	HA		WM	
	Friction Coeff. (μ)	Wear rate, 10^{-5} ($mm^3(Nm^{-1})$	Friction Coeff (μ)	Wear rate, 10^{-5} ($mm^3(Nm)^{-1}$)
50	0.2340	0.98	0.3734	3.25
70	0.2856	1.4	0.4247	3.87
90	0.3312	1.63	0.4369	4.22
110	0.3786	1.78	0.4832	4.45

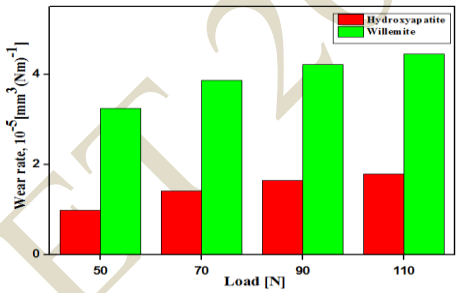

Fig. 7 Wear rates of HA and WM

.

Also, Theoretical calculations were used to calculate wear rate of specimens.

Table. 3. Experimental wear depth

Samples	Load (N)	Total mass loss grams	Depth of Wear in mm
HA	50	0.001	6.25
	70	0.002	12.51
	90	0.003	18.17
	110	0.004	25.03
WM	50	0.003	18.85
	70	0.005	31.42
	90	0.007	43.99
	110	0.009	56.56

Table 3. showed total mass loss in grams of the specimen which were taken by performing experimentation on Tribometer and wear depth.The volume loss of specimen can be calculated using equation (1)

$$Volume = \frac{Mass\ loss}{Density\ of\ pin} \quad \ldots\ldots\ldots\ldots (1)$$

Now, Depth of wear rate of specimen was calculated by using equation (2),

$$Volume\ of\ pin = \pi * r^2 * h \quad \ldots\ldots\ldots\ldots (2)$$

Where r = Radius of pin, h= height of pin. Hence, it's possible to calculate the depth of wear experimentally.

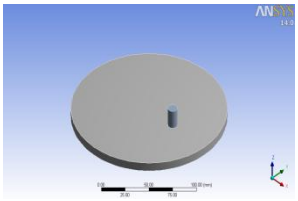

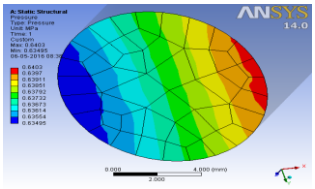

Fig. 9 3-D solid model of Tribometer
Fig. 10 Contact pressure distribution in an interfacing of pin and disc

NUMERICAL ANALYSIS USING FEA:

A static analysis using Ansys calculated the effects of steady loading conditions on a structure. The static analysis determined the displacements, pressure, stresses, strains, and forces in structures or components caused by loads that did not induce significant inertia and damping effects. The flow chart of the steps used for static analysis, consisting of a series of steps were shown in Fig. 9 and Table. 4 consist material property used for analysis.

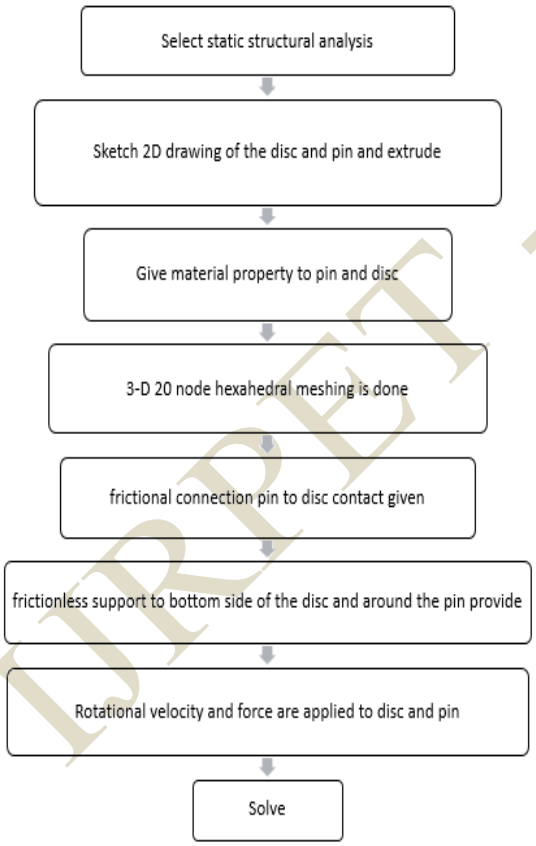

Fig.8 Flow chart of the static structural analysis

Table. 4 Material property used for analysis

Parameter	HA	WM	Gray cast iron
Young's modulus	40 GPa	37.5 GPa	110 GPa
Poisson's ratio	0.28	0.3	0.3
Density	2.034 g/cm3	2.026 g/cm3	6.850g/cm3

The final CAD model is prepared from the dimensions that were taken from Tribometer test setup.First disc has created with 165 mm diameter with 8 mm thick and pin of 10 mm diameter and 20 mm thick.

Fig. 9 show the solid model of Tribometer in an X-Y plane. From this, we observe that a pin was perfectly flat contact with the rotating disc at 70 mm track diameter and Fig. 10 show the contact pressure distribution on an interfacing surface of pin in contact with the disc. Form above solution, we got maximum pressure value. Substituting this Value in Archard equation [44], we got the depth of wear.The depth of wear rate was calculated using equation given below: (3)

$$Depth of\ wear,\ h = K \times P \times S \quad \text{.....(3)}$$

Where,
K = wear coefficient in m2/N,
P = contact pressure distribution in N/m2,
S = sliding distance in meter (1000m).

Wear coefficientwas calculated using equation (4),

$$Wear\ coefficient = \frac{V'}{S \times F_n} \quad \text{.....(4)}$$

Where,
V'= measured wear volume,
S =sliding distance,
Fn= applied load.

Now, putting all these values in equation (4) we got,

Table. 5 Numerical wear depth

Samples	Load N	Maximum Contact pressure in MPa	Wear coefficient m2/N	Depth of Wear in mm
HA	50	0.6403	$9.8328*10^{-15}$	6.29
	70	1.0324	$1.40469*10^{-14}$	14.5
	90	1.3273	$1.63880*10^{-14}$	21.75
	110	1.5823	$1.78778*10^{-14}$	28.28
WM	50	0.6701	$2.96150*10^{-14}$	19.84
	70	0.9648	$3.52555*10^{-14}$	34.01
	90	1.2096	$3.83898*10^{-14}$	46.43
	110	1.4843	$4.03840*10^{-14}$	59.88

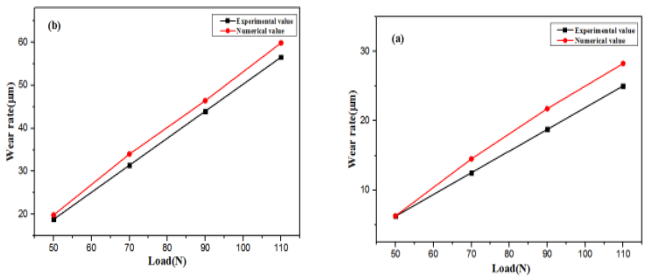

Fig. 11 Comparison of Experimental and Numerical results (a) HA and (b) WM

From Fig. 12, it was observed that no significant difference found between numerical and experimental result. In numerical result may have errors probably aroused in making modelling, meshing strategy and may be due to operator skill, but this numerical result has many advantages compared to experimentation. Numerical result was useful to give a result at various times that were difficult, expensive or time consuming to study using experimental techniques. Numerical predictions for wear rate were useful for all desired quantities, high resolution in time, portable, easy to modify and cheap in cost. Also, it is fast and used for multiple purposes and can be used to compare with experimental results. The numerical analysis does not replace measurement completely, but reduces amount of experimentation and cost significantly.

CONCLUSIONS

In the present research work HA and WM were successfully prepared by the conventional sol-gel auto combustion and sol-gel method respectively. We were able to prepare pin of both materials using acrylic repair material. EDS studies confirmed the presence of HA and WM. The friction and wear properties of HA and WM were studied in dry medium. Friction test showed that the friction coefficient of HA was smaller than WM. The friction coefficient of both materials goes on increasing as load increases. The wear rate of HA was much lower than the WM. As the load increased wear rate of HA and WM goes on increase. It was observed that there was no significant difference in between wear depth calculated by experimentally and numerically. Hence, it was concluded that HA is potentially applicable as a friction material in engineering application also, in biomedical application than WM.

REFERENCES

1) A. Bigi, E. Boanini, K. Rubini, Hydroxyapatite gels and nanocrystals prepared through a sol–gel process, J. Solid State Chem. 177(2004) 3092–3098.
2) M. Vallet-Regi, J.M. Gonzalez-Calbet, Calcium phosphates as substitution of bone tissues, Prog. Solid State Chem. 32(2004) 1–31.
3) S.I. Roohani-Esfahani, S. Nouri-Khorasani, Z.F. Lu, M.H. Fathi, M. Razavi, R.C. Appleyard, H. Zreiqat, Modification of porous calcium phosphate surfaces with different geometries of bioactive glass nanoparticles, Mater. Sci. Eng. C 32(2012) 830–839
4) B. Viswanath, N.Ravishankar, Controlled synthesis of plate-shaped hydroxyapatite and implications for the morphology of the apatite phase in bone, Biomaterials. 29(2008) 4855–4863.
5) W.A. Curtin, B.W. Sheldon, CNT-reinforced ceramics and metals, Mater, today 7(2004) 44-49
6) Suchanek W, Yoshimura M (1998) Processing and Properties of Hydroxyapatite-Based Biomaterials for Use as Hard Tissue Replacement Implants. Journal of Materials Research 13(1):94–117.
7) H. Zhou, J. Lee, Acta Biomater.Nanoscale hydroxyapatite particles for bone tissue engineering, 7(2011) 2769-2781.
8) J.S. Cho, H.S. Kim, S.H. Um, S.H. Rhee, J. Biomed. Mater. Res., B 101B (2013)
9) T. Hara, K.Mori, T.Mizugaki, K.Ebitani, K.Kaneda, Tetrahedron Lett. 44(2003) 6207- 6210.
10) P.C. Lin, S.C.Lin, W.H.Hsu, J.Chin.Inst.Chem.Eng. 39(2008) 389–398.
11) G. Ciobanu, M.Harja, L.Rusu, A.M.Mocanu, C.Luca Korean J.Chem.Eng. 31(2014) 1021– 1027.
12) S. Ezhaveni, R. Yuvakkumar, M. Rajkumar, N. M. Sundaram, V. Rajendran, J.Nanosci.Nanotechnol. 13(2013) 1631–1638.
13) K.M. Knowles, F.S.H.B. Freeman, Microscopy and microanalysis of crystalline glazes, J. Microsc. 215(2004) 257–270.
14) H. Cui, M. Zayat, and D. Levy, "Nanoparticle synthesis of willemite doped with cobalt ions (Co0.05Zn1.95SiO4) by an epoxide- assisted sol-gel method," Chemistry of Materials, 17, 22, 5562–5566, 2005.
15) Y. Mao, J. Y. Huang, R. Ostroumov, K. L. Wang, and J. P. Chang, Synthesis and luminescence properties of Erbium-doped Y2O3 nanotubes, The Journal of Physical Chemistry C, 112, 7, 2278–2285, 2008.
16) B. Chandra Babu, S. Buddhudu, Dielectric properties of Willemite -Zn2SiO4 nano powders by sol-gel method, Physics Procedia 49(2013) 128 – 136.
17) T. K. GunduRao , NiloF.Cano,Betzabel N. Silva-Carrera, Reinaldo M. Ferreira , Henry Javier Ccallata, Shigueo Watanabe,Centers responsible for the TL peaks of willemite mineral estimated by EPR analysis,Journal of Luminescence,177,(2016) 139–144.
18) H. Chander, Mater. Sci. Eng., R 49(2005) 113–155.
19) H.A. Höppe, Angew. Chem. Int. Ed. 48(2009) 3572–3582.
20) J. Shen, L.D. Sun, C.H. Yan, Dalton Trans. 42(2008) 5687–5697.
21) Bharat.Bhusan, Introduction to Tribology, 2nded John Wiley & Sons, e-book, 2013, 1.
22) Qian Zhao, YalongShen, MeiruJi, Lei Zhang, Tingshun Jiang, CangshengLi.z,Effect of carbon nanotube addition on friction coefficient of

nanotubes/hydroxyapatite composites , Journal of Industrial and Engineering Chemistry 20(2014) 544–548.
23) Zhi Lu, Yong Liu, Bowei Liu, Meiling Liu, Micro-tribological properties of hydroxyapatite-based composites in dry sliding,Materials and Design 46(2013) 794–801.
24) J. Zheng, Y. Li, M.Y. Shi, Y.F. Zhang, L.M. Qian, Z.R. Zhou, Microtribological behaviour of human tooth enamel and artificial hydroxyapatite, Tribology International. 63(2013) 177–185.
25) R. Murugan,S.Ramakrishna, Production of ultra-fine bioresorbable carbonated hydroxyapatite, ActaBiomater. 2(2006) 201–206.
26) M.H. Fathi, A.Hanifi, V.Mortazavi, Preparation and bioactivity evaluation of bone-like hydroxyapatite nanopowder, J.Mater.Process. Technol. 202(2008) 536–542.
27) G.C. Koumoulidis, A.P.Katsoulidis, A.K.Ladavos, P.J.Pomonis, C.C. Trapalis,
28) A.T.Sdoukos, T.C.Vaimakis, Preparation of hydroxya-patite via microemulsion route, J.Colloid Interface Sci. 259(2003) 254–260.
29) Z. Zou, K.Lin, L.Chen, J.Chang, Ultra fast synthesis and characterization of carbonated hydroxyapatite nanopowders via sonochemistry- assisted micro wave proces, Ultrason.Sonochem. 19(2012) 1174–1179.
30) S. Lala, S.Brahmachari, P.K.Das, D.Das, T.Kar, S.K.Pradhan, Biocompatible nanocrystalline natural bone like carbonated hydroxyapa- tite synthesized by mechanical alloying in a record minimum time, Mater. Sci.Eng.C 42(2014) 647–656.
31) A.G. Merzhanov, 40 years of SHS: A lucky Star of Scientific Discovery,Bentham Science, e-book, , 2012,112.
32) S.T. Aruna, Solution combustion synthesis – an overview, in: M. Lackner (Ed.),
33) Combustion Synthesis: Novel Routes to Novel Materials, Bentham Publishers, 2010, 206–221.
34) R. Pozas, V.M. Orera, M. Ocana.Journal of the European Ceramic Society. 25(2005) 3165–3172.
35) Meili Zhang, WanyinZhai, Jiang Chang. J Mater Sci: Mater Med (2010) 21:1169–1173.
36) Chundong Li, Zhiqiang Liang, Haiying Xiao, Yiyong Wu, Yong Liu. Materials Letters 64 (2010) 1972–1974.
37) L. Reynaud, C. Brouca-Cabarrecq and A. Mosset. Materials Research Bulletin, 31, 9, (1996) 1133-1139.
38) MasafumiTakesue, Hiromichi Hayashi, Richard L. Smith, Jr. Progress in Crystal Growth and Characterization of Materials 55(2009) 98-124.
39) Tanaji V Kolekar, Nanasaheb D Thorat, Hemraj M Yadav, Veeresh T Magalad, Mahesh Shinde, Sneha S Bandgar, Jin H Kim and Ganesh L Agawane,Nanocrystalline hydroxyapatite doped with aluminium: A potential carrier for biomedical applications, Ceramic international vol 42, issue 4(2016) 5304-5311.
40) Mu-Tsun Tsai, Jun-Min Wu, Yu-Feng Lu, Hen-Chia Chang, Synthesis and luminescence characterization of manganese-activated Willemite gel films,Thin Solid Films 520 (2011) 1027–1033.
41) BulentOzturk, FazilArslan, Sultan Ozturk, Hot wear properties of ceramic and basalt fiber reinforced hybrid friction materials,Tribology International 40(2007) 37–48.
42) L.A.Azaroff, elements of X-ray crystallography, Mc-Graw-Hill, New York,1968.38-42.
43) S.J.Kalita, S.Bose, H.L.Hosick, A.Bandopadhyay, Biomaterials 25(2004) 23-31.
44) Samar J. kalita, HimeshA.Bhatt, Material science and engineering 27(2007) 837-848.
45) N. NayebPashaee, A.M. Aarabi, H. Sarpoolaky, H. Vafaeenezhad, Metall. Mater. Eng. Vol 21 (2) (2015) 89-99.
46) V. Hegadekatte, S. Kurzenhauser, N. Huber, O. Kraft, A predictive modeling scheme for wear in tribometers, Tribology International. 41(2008) 1020-1031.